Major Histocompatibility Complex Class II Compartments in Human and Mouse B Lymphoblasts Represent Conventional Endocytic Compartments

Monique J. Kleijmeer,* Stanislaw Morkowski,‡ Janice M. Griffith,* Alexander Y. Rudensky,‡§ and Hans J. Geuze*

*Department of Cell Biology, School of Medicine and Institute of Biomembranes, Utrecht University, 3584 CX Utrecht, The Netherlands; and ‡Department of Immunology and §Howard Hughes Medical Institute, University of Washington, School of Medicine, Seattle, Washington 98105

Abstract. In most human and mouse antigen-presenting cells, the majority of intracellular major histocompatibility complex (MHC) class II molecules resides in late endocytic MHC class II compartments (MIICs), thought to function in antigen processing and peptide loading. However, in mouse A20 B cells, early endocytic class II-containing vesicles (CIIVs) have been reported to contain most of the intracellular MHC class II molecules and have also been implicated in formation of MHC class II–peptide complexes. To address this discrepancy, we have studied in great detail the endocytic pathways of both a human (6H5.DM) and a mouse (A20.A^b) B cell line. Using quantitative immunoelectron microscopy on cryosections of cells that had been pulse–chased with transferrin-HRP or BSA-gold as endocytic tracers, we have identified up to six endocytic subcompartments including an early MIIC type enriched in invariant chain, suggesting that it serves as an important entrance to the endocytic pathway for newly synthesized MHC class II/invariant chain complexes. In addition, early MIICs represented the earliest endocytic compartment containing MHC class II–peptide complexes, as shown by using an antibody against an abundant endogenous class II–peptide complex. The early MIIC exhibited several though not all of the characteristics reported for the CIIV and was situated just downstream of early endosomes. We have not encountered any special class II-containing endocytic structures besides those normally present in nonantigen-presenting cells. Our results therefore suggest that B cells use conventional endocytic compartments rather than having developed a unique compartment to accomplish MHC class II presentation.

MAJOR histocompatibility complex (MHC)[1] class II molecules expressed at the surface of antigen-presenting cells (APCs) such as B lymphocytes, dendritic cells, and macrophages present bound peptides derived from exogenous antigens to CD4-positive T lymphocytes. The antigens are internalized by fluid-phase- and receptor-mediated endocytosis or by phagocytosis and are proteolytically cleaved in endocytic compartments to reveal small fragments that can associate with the binding groove of MHC class II molecules (for reviews see 9, 14, 62). Peptide binding occurs predominantly to newly synthesized rather than to surface-derived class II molecules (3, 10, 34). Delivery of class II molecules from the biosynthetic to the endocytic pathway requires their association with invariant chain (I-chain; 9, 56). Class II/I–chain complexes are thought to be transported from the TGN to late endocytic compartments (10, 32, 34, 36, 37, 60) or (in addition) to earlier endosomes either directly or via the plasma membrane (6, 8, 26, 48, 58). Upon arrival in endosomes, the I-chain is rapidly degraded starting from the luminal COOH terminus (47). A portion of the I-chain, CLIP (class II-associated I-chain peptides) remains transiently bound in the class II groove until it is exchanged for antigenic peptide, a process that is facilitated by the class II-related molecule human leukocyte antigen (HLA)-DM (H2-M in mice; 11, 45). It is not precisely known at which site(s) in the endocytic pathway peptide binding takes place. Peptide-loaded class II molecules are transported to the plasma membrane via largely unknown pathways (59), one of which is by exocytosis of MHC class II-enriched

Address all correspondence to Hans J. Geuze, Medical School, Department of Cell Biology, AZU H02.314, Heidelberglaan 100, 3584 CX Utrecht, The Netherlands. Tel.: (31) 30-2507652. Fax: (31) 30-2541797. E-mail: h.j.geuze@lab.azu.nl

1. *Abbreviations used in this paper*: APC, antigen-presenting cell; CD, cation dependent; CIIV, class II-containing vesicle; EE, early endosome; HLA, human leukocyte antigen; I-chain, invariant chain; IEM, immunoelectron microscopy; LAMPS, lysosome-associated membrane proteins; MPR, mannose 6-phosphate receptor; LE, late endosome; MHC, major histocompatibility complex; MIIC, MHC class II-enriched compartment; Tf, transferrin.

compartments (MIICs; 43, 64). Thus, there is abundant evidence for the crucial role of the endocytic pathway in class II antigen presentation.

At steady state, APCs harbor a major pool of their intracellular class II molecules in endocytic compartments, morphologically reminiscent of multivesicular late endosomes and lysosomes and which are collectively called MIICs (20, 34, 35, 37). Recently, several subtypes of MIICs have morphologically been distinguished, including those containing internal vesicles and membrane sheets, termed multivesicular and multilaminar MIICs, respectively (38). In a recent study on human B cells, an MIIC subtype was identified containing abundant I-chain and only a few vesicles. This so-called early MIIC was proposed to be a precursor compartment of the classical MIICs (17). Cell fractionation and immunoelectron microscopy (IEM) suggested that these early MIICs represent the main entry site of newly synthesized class II molecules into the endocytic pathway (17, 38). These results were broadly consistent with those of Castellino and Germain (6), who showed that class II/I–chain complexes enter early endocytic compartments. Experiments with exogenous tracers have shown that multivesicular MIICs are positioned earlier in the endocytic pathway than multilaminar MIICs and gradually mature into the latter type (24). It is not yet clear how MIICs relate to classical endocytic compartments present in non-APCs and whether APCs have developed special endocytic structures dedicated to class II functioning besides other endosomes (53, 65). A detailed morphological description of the entire endocytic pathway in an APC and the distribution of class II herein could help answer these questions.

In non-APCs, at least four types of endocytic structures have been distinguished on the basis of endocytic kinetics and differential distribution of marker proteins, i.e., primary endocytic vesicles, early endosomes (EEs), late endosomes (LEs), and lysosomes (for review see 29). However, due to the plasticity of the endocytic system, no clear separation between EEs, LEs, and lysosomes can be made. Nevertheless, several markers have proven to be useful to make operational distinctions. Thus, the presence of the transferrin (Tf) receptor and internalized Tf is commonly used to identify EEs, while the cation-independent and -dependent (CD) mannose-6-phosphate receptors (MPRs), involved in the delivery of newly synthesized lysosomal enzymes to the endocytic pathways, are widely used as discriminative markers present in LEs but absent from lysosomes (16, 19, 25). Lysosomes can also be recognized by the presence of lysosomal enzymes and lysosome-associated membrane proteins (LAMPS; for review see 21). However, many cell types show hardly any MPRs in endocytic structures by IEM, while LAMPS and lysosomal enzymes are present in typical dense lysosomes as well as in LEs (16, 25). Both with IEM and cell fractionation, MIICs do not contain significant amounts of TfRs but are enriched in lysosomal enzymes and LAMPs and therefore are categorized as late endocytic or (pre)lysosomal structures (37, 41, 57, 60).

In B cells and macrophages, MIICs have been suggested to represent peptide-loading compartments (20, 31, 41, 51, 60, 65). In accordance with this function, MIICs contain high levels of HLA-DM molecules (35, 39, 52). However, several other studies have shown that class II molecules can already acquire peptide in early endocytic structures (6, 13, 18). Using free-flow electrophoresis of mouse A20 B lymphoma cells, Amigorena and coworkers (1, 2) and Pierre et al. (39) have described a distinct class II peptide-loading compartment named class II-containing vesicle (CIIV), which was thought to be different from classical endosomes. The relation between CIIVs and MIICs is not yet clear. The present study presents a detailed IEM characterization of the endocytic pathways in a human B cell line and in the murine A20 cells and addresses the question of whether these APCs contain specialized and/or conventional class II-containing endocytic compartments. Using quantitative immunogold labeling and a recently improved cryosectioning technique (28), we studied the progression of internalized tracers through the endocytic pathway and subdivided the endocytic pathway into up to six subcompartments. Class II molecules distributed to all types of endocytic compartments downstream of the main Tf-containing EEs in both human and mouse B cells. Using an antibody selectively recognizing an abundant class II–peptide complex (43, 50), we found that early MIICs seen just downstream of EEs represent the earliest endocytic structures exhibiting class II–peptide complexes. Our observations do not support the existence of a distinct set of endocytic organelles specialized in class II functioning.

Materials and Methods

Cells

The human 6H5.DM cell line was obtained by transfection of the human B-LCL cell line Sweig with I-A^b α and β genes and HLA-DM genes as described before (43). The mouse lymphoblastoid cell line A20 was transfected with the expression constructs containing cDNA encoding I-A^b α- and β-chains driven by the human β actin promotor and neomycin- and hygromycin-resistance genes. The expression constructs were identical to those used to obtain 6H5.DM cells. 48 h after electroporation, the cells were subjected to selection in culture medium containing 3 mg/ml G418 (GIBCO BRL, Gaithersburg, MD) and 1.2 mg/ml hygromycin B (Boehringer Mannheim, Indianapolis, IN). Stable transfectants (A20.A^b) were cloned by limiting dilution and screening for surface expression of I-A^b molecules by flow cytometry using mAb Y3P (12). Both cell lines were maintained in RPMI 1640 supplemented with 5% FCS, 200 mM L-glutamine, 100 U/ml penicillin and streptomycin, 10 mM Hepes, 1 mM sodium pyruvate, and 5×10^{-5} M β-mercaptoethanol (all from GIBCO BRL) in 5% CO_2 atmosphere at 37°C (sRPMI).

Immunoelectron Microscopy

Cells were prepared for ultrathin cryosectioning and immunogold labeled as described (15, 54). Briefly, cells were fixed in 2% paraformaldehyde and washed in PBS and PBS/0.02 M glycine. Cell pellets were embedded in 7.5% gelatin, which was solidified on ice and cut into small blocks. After infiltration with 2.3 M sucrose for 3 h at 4°C, the blocks were mounted and frozen in liquid nitrogen. Ultrathin cryosections were embedded in a mixture of sucrose and methyl cellulose according to a novel procedure allowing a better visualization of membranes (28). Ultrathin cryosections were single immunolabeled with 10-nm gold particles or double immunolabeled with 5- and 10-nm or 10- and 15-nm protein A–gold particles.

Antibodies

For IEM we used rabbit polyclonal antisera specific for human HLA-DR α-chain (34), human I-chain NH_2 and COOH terminus (11), human HLA-DMα (FS2; 52), human LAMP-1 (61), human CD-MPR (MSC1; kind gift of Dr. K. von Figura, Georg-August University, Göttingen, Germany; 25), mouse H-2Mb (K553 in biotinylated form; kind gift of Dr. L. Karlsson, Johnson Pharmaceutical Research Institute, Scripps Research Institute,

La Jolla, CA,), mouse LAMP-1 (7), HRP (p7899; Sigma Chemical Co, St. Louis, MO), mouse I-chain luminal part (S22; kind gift of Dr. N. Koch, University of Bonn, Bonn, Germany; 27), and biotin (Rockland, Gilbertsville, PA). In addition, we used a rat mAb specific for the cytoplasmic tail of mouse I-chain (In-1; 26), mouse mAbs specific for mouse cathepsin D (generous gift of Dr. K. von Figura), I-$A^{b/d}$/I-E (4), and for Eα(DRα)52-68 peptide bound to I-A^b called YA*e* (12).

Internalization of Tf-HRP and BSA-Gold

Tf was coupled to HRP as described (55). Tf-HRP was added to 6H5.DM or A20.A^b cells at a concentration of 25 μg/ml for 3 or 10 min at 37°C. The cells were washed in cold medium and fixed as described above. BSA conjugated to 5-nm colloidal gold particles (54) was used in pulse–chase experiments to label endocytic compartments. Cells were either incubated with BSA-gold for 3 or 10 min at 37°C, washed extensively in cold medium, and fixed (as described above), or incubated for 10 min at 37°C, washed extensively, chased for 20 or 50 min at 37°C, and then fixed. Ultrathin cryosections of cells incubated with Tf-HRP, were immunolabeled with anti-HRP antibody and 10-nm gold particles. Of both 3 and 10 min time points, 20 cell profiles were randomly selected in the cryosections, and gold particles were assigned to the various types of endocytic compartments (see Results and Tables I and II). For each compartment, the percentage of the total immunogold was calculated. The same was done with 5-nm BSA-gold particles internalized after 3- and 10-min pulse, and 10-min pulse plus 20- or 50-min chase. In the same sections, the contribution of each of the types of endocytic compartments to the total number of endocytic compartments per cell profile was determined. In 6H5.DM and A20.A^b cells six and five, respectively, different types of endocytic compartments were described morphologically and ordered according to their position in the endocytic pathway (see Results). The distinctive morphological characteristics of each of these compartments were then used to study the distribution of markers of interest. Of each immunolabeling, 20 cell profiles were evaluated quantitatively. Gold particles were assigned to a compartment when lying within a distance of twice the particle size from the membrane. Gold particles present on other, nonendocytic organelles were not taken into account. Background labeling using an irrelevant antibody was negligible.

Results

Since no detailed morphological characterization of the endocytic system in B lymphocytes has been described so far, we have first analyzed the endocytic compartments in the human B cell line 6H5.DM and the mouse B cell line A20.A^b. The A20 cell line has been used extensively in biochemical fractionation studies (1, 2, 39) but has not been studied morphologically in great detail. We have used Tf conjugated to HRP as a receptor ligand or 5-nm BSA-gold particles as fluid-phase endocytic tracer to study the progression of the internalized tracers through the endocytic pathway in thawed cryosections of 6H5.DM and A20.A^b cells. We took advantage of the improved cryosection morphology (28), which enabled us to subdivide the endocytic pathway into a series of compartments according to morphological and endocytic characteristics. Next, we studied the distribution of a variety of markers of the class II pathway in these compartments by IEM.

Kinetics of Tracer Uptake in 6H5.DM Cells

Examination of ultrathin cryosections of 6H5.DM cells pulsed with either Tf-HRP or with 5-nm BSA-gold particles for 3 or 10 min, or pulsed for 10 min and chased for 20 or 50 min, revealed six types of endocytic compartments. Each of the compartments displayed distinct morphological features (Figs. 1 and 2; see also the schematic representation of the various compartments in Fig. 3 and Table I). Fig. 1 shows several compartments in cells that had taken up Tf-HRP (Fig. 1, *A–D*) or BSA-gold (Fig. 1, *E* and *F*). Tf-HRP, detected by immunogold labeling, was found primarily in small clathrin- and nonclathrin-coated vesicles and tubules, which together were termed endocytic compartment type 1 (Fig. 1, *A* and *B*; see numbering on the figures). Additional compartments displaying Tf-HRP showed an extended straight or curved tubular morphology with occasional internal vesicles (type 2; Fig. 1, *C* and *D*) or were typically irregularly shaped, with a few internal vesicles (type 3; Fig. 1, *B* and *D*). Type 2 and 3 compartments could also easily be recognized by an electron-lucent area inside the curvature of the compartment (Figs. 1, *C* and 2, *A* and *B*). Tf-HRP was not found in compartments other than types 1–3. After 3 min of uptake, the majority of BSA-gold particles was detected in types 1 and 2 (not shown) and to some extent in type 3 compartments (Fig. 1 *E*). Type 4, 5, and 6 compartments showed barely any BSA-gold at 10 min (Fig. 1 *F*) but were reached by BSA-gold after prolonged time periods of uptake (30–60 min, not shown).

For a quantitative evaluation of endocytic tracers present in each of the six morphologically distinguishable subcompartments, Tf-HRP immunogold labeling and BSA-gold particles were counted in 20 random cell profiles at each uptake time (Table I). After 3 min, 73% of the Tf-HRP was detected in type 1, 22% in type 2, and 5% in type 3 compartments. The distribution of Tf-HRP was not significantly different after 10 min of uptake. This result indicates that Tf-HRP is not transported much farther into the endocytic pathway and marks the steady-state recycling pathway of the Tf receptor. We conclude that type 1 and 2 compartments are the classical EEs in these cells.

Analysis of BSA-gold uptake revealed that immediately after 3 and 10 min about one third of the total internalized tracer was present in type 3 compartments. The labeling further increased after 10 plus 20 min, with a simultaneous decrease in types 1 and 2. This indicates that type 3 compartments were positioned downstream of types 1 and 2. At 20 and 50 min chase, type 4, 5, and 6 compartments were sequentially reached by BSA-gold, indicating that these compartments were situated in this order later in the endocytic pathway. Type 4 compartments contained internal vesicles reminiscent of classical multivesicular endosomes in most cell types, type 6 displayed internal membrane sheets, whereas type 5 had an intermediate morphology. Types 4, 5, and 6 did not contain detectable internalized Tf-HRP at any time, which positioned them downstream of recycling EEs. Type 4, 5, and 6 compartments represented MIICs (see below) as defined originally (37) and together comprise the late endocytic compartments (Table I). Both tracer kinetics and morphology indicated that type 3 compartments represent a transitional stage between the early type 2 and the later type 4 compartments.

Quantitative Distribution of Class II, I-Chain, HLA-DM, and YAe in 6H5.DM Cells

Human 6H5.DM cells displayed several useful features for a study on class II distribution. First, they expressed I-A^b molecules, which are able to bind peptide derived from the endogenous DR α-chain. These DRα52-68/I-A^b peptide complexes are recognized by mAb YA*e* (33), which can be

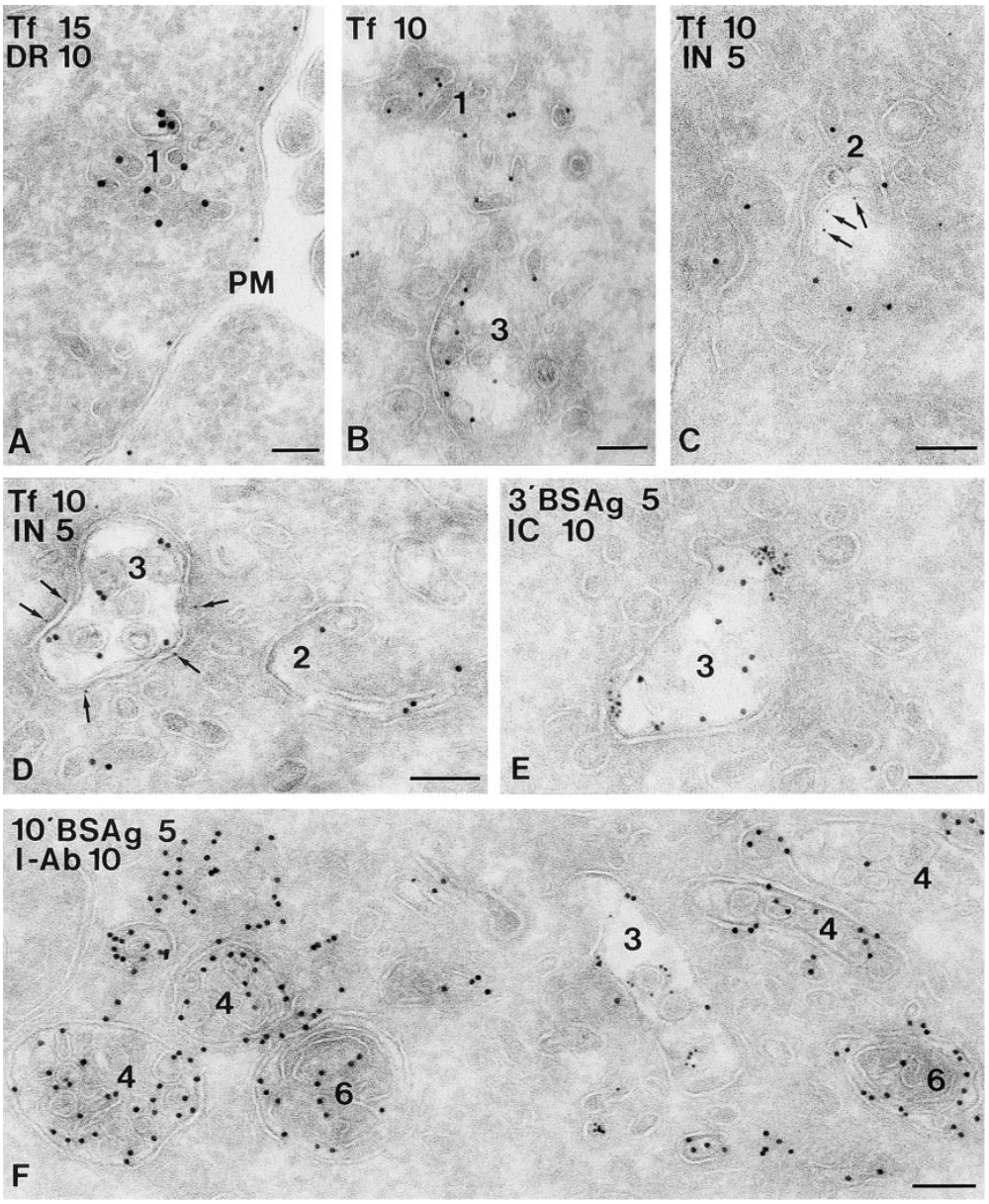

Figure 1. Endocytic compartments in 6H5.DM cells. Cells were incubated with Tf-HRP (*Tf*) for 3 or 10 min or with 5 nm BSA-gold (*BSAg*) for 3 or 10 min. Tf was detected with an HRP antibody (15- or 10-nm gold particles, *A*, *B*, *C*, and *D*, respectively). In addition, ultrathin cryosections were immunolabeled with antibodies specific for HLA-DR (*A*), I-chain NH_2 terminus (*C* and *D*, *IN*) and I-chain (*E*, *IC*), or I-A^b (*F*). The distinct types of endocytic compartments are numbered 1 through 6. Tf is present in small vesicles and tubules (*A* and *B*), whereas 10-nm immunogold particles for DR are present only on the plasma membrane (*A*, *PM*). Type 2 compartments containing Tf are shown in *C* and *D* and characterized by an elongated tubular morphology with few internal vesicles. The typical electron lucent area can be seen in the curvature of the tubule (*C*). Type 3 compartments are shown in *B*, *D*, *E*, and *F*, and exhibit an irregular morphology and an electron lucent content with some internal vesicles. The type 3 compartment contains Tf labeling (*C* and *D*) and also 5 nm BSAg after 3 and 10 min of uptake (*E* and *F*, respectively). IN labeling is present on both the type 2 (*C*) and type 3 compartment (*D*). Immunolabeling for the luminal epitope of I-chain (*IC*) is abundant on the type 3 compartment (*E*). Multivesicular type 4 and multilaminar type 6 compartments (*F*) are negative for 5 nm BSAg after 10 min of uptake. Colocalization of I-A^b and BSAg is seen only in the type 3 compartment. Bar, 100 nm.

used in IEM. In addition, the high level of HLA-DM expression caused an increased number of peptide-loaded class II molecules (42 and M.J. Kleijmeer, unpublished observations). Immunolabeling patterns for the various markers of the class II pathway in 6H5.DM cells are illustrated in Figs. 1 and 2 and quantitatively represented in Fig. 3 *A*. Both HLA-DR and I-A^b molecules were most prominently present in type 4, 5, and 6 compartments (illustrated for DR in Fig. 2, *A*, *B*, and *D*, and for I-A^b in Fig. 1 *F*) and to a much lower extent in type 3 (Fig. 2 *A*). As in previous studies, types 4, 5, and 6 MIICs contained LAMP-1, as shown for a type 6 multilaminar MIIC in Fig. 2 *A*, and were devoid of MPR (Fig. 2 *C*). DR and I-A^b were undetectable in type 1 (Fig. 1 *A*) and type 2 compartments and were present at low levels in type 3 compartments. In contrast, labeling for both the NH_2 and COOH terminus of I-chain was low or undetectable in types 5 and 6 but was high in types 3 and 4 (Figs. 1, *D* and *E* and 2 *B*). A low but significant amount was also detectable in type 2 compartments (Figs. 1 *C* and 2 *B*). Almost 60% of the total COOH terminus labeling was contained in type 3 compartments. Type 3 compartments showed all of the characteristics of early MIICs as defined previously (17), being small, irregularly shaped multivesicular structures, often showing an electron lucent area enclosed in the curvature of the compartment. In type 4, NH_2 terminus labeling was about the same as in type 3, but COOH terminus labeling was less than half of that in type 3. This may reflect the degradation of I-chain, which starts at the COOH terminus. As has been observed before (35, 52), DM was

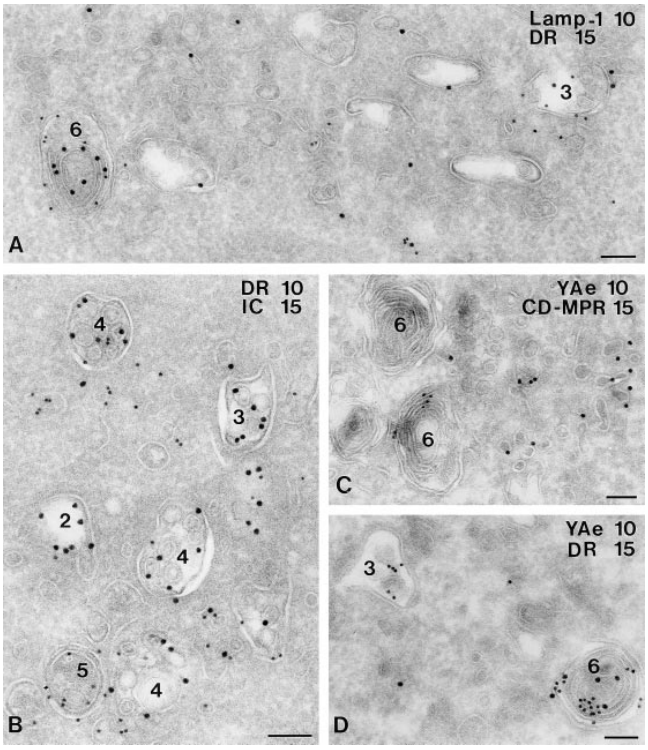

Figure 2. Characterization of MIICs in 6H5.DM cells. Ultrathin cryosections of 6H5.DM cells were immunolabeled with antibodies specific for LAMP-1 (*A*), I-chain COOH terminus, (*B*), CD-MPR (*C*), and peptide-loaded I-A^b (*C* and *D*, YA*e*). LAMP-1 (10-nm gold particles) is present on a multilaminar type 6 compartment (*A*), which also contains DR labeling (15-nm gold particles). In addition, both LAMP-1 and DR are found on a type 3 compartment, although to a smaller extent than on the type 6 compartment. I-chain COOH terminus labeling is restricted to type 2, 3, and 4 compartments (*B*), whereas DR is present in the multivesicular type 4 and more abundantly on the mixed type 5 compartment. Two typical type 6 compartments are shown in *C*; one of them shows labeling with YA*e* (10-nm gold particles). CD-MPR is absent from the type 6 compartments; labeling of CD-MPR (15 nm) is restricted to small, dense vesicles. YA*e* labels both on a type 3 and type 6 compartment (*D*). Bars, 100 nm.

strongly enriched in type 6 multilaminar MIICs (47%). Of the total peptide-loaded I-A^b molecules (YA*e*), 11% was present in type 3 whereas most YA*e* labeling was found in type 5, the intermediate MIICs. YA*e* labeling was absent from types 1 and 2. Thus, type 3/early MIICs were the earliest endocytic compartments showing YA*e* epitope (Fig. 2 *D*) and therefore may represent the earliest loading compartment, situated just downstream of the major Tf-containing EEs (types 1 and 2). Most of the YA*e*, however, was found in later type 4, 5, and 6 compartments, which also contained most of the HLA-DM and class II molecules (Fig. 2 *C*).

Kinetics of Tracer Uptake in A20.A^b Cells

By morphology, A20.A^b cells showed endocytic compartments very similar to those of 6H5.DM cells (Figs. 4 and 5). However, the typical multilaminar type 6 was not prominently present, whereas the intermediate type 5 was absent. In their place, a dense compartment with some internal membranes was found, which we indicated as type 5/6 (Figs. 4 *E* and 5, *A* and *B*). As in 6H5.DM cells, Tf-HRP was mainly found in types 1 and 2 and was absent from the multivesicular type 4 (Fig. 4 *C*). Type 1, 2, and 3 compartments were reached by internalized BSA-gold particles after 3 min of uptake (Fig. 4, *A* and *B*). Type 5/6 compartments were not reached by BSA-gold before 10 min of uptake but obtained BSA-gold only after 10-min pulse and 20- or 50-min chase (not shown). As in 6H5.DM cells, type 2 and 3 often showed characteristic electron lucent areas (Figs. 4, *C* and *D,* and 5 *C*). Notably, A20.A^b cells contained considerably fewer endocytic compartments than 6H5.DM cells, i.e., 10 versus 20 per random cell profile, respectively.

Table I. Quantitative Analysis of Tf-HRP and BSA-Gold Uptake in 6H5.DM Cells

6H5DM	Type 1	Type 2	Type 3	Type 4	Type 5	Type 6
3 min Tf-HRP	73	22	5	–	–	–
10 min Tf-HRP	79	18	3	–	–	–
3 min BSA-gold	47	24	29	–	–	–
10 min BSA-gold	35	32	33	–	–	–
10 + 20 min BSA-gold	10	10	40	37	3	–
10 + 50 min BSA-gold	2	2	7	49	31	9

6H5.DM cells were incubated at 37°C with Tf-HRP for 3 and 10 min or pulse–chased with 5-nm BSA-gold particles for the indicated time periods. Tf-HRP was visualized on ultrathin cryosections with an HRP antibody and 10-nm gold particles. For each incubation, 20 cell profiles were randomly selected, and gold particles labeling Tf-HRP were assigned to a compartment when within 20 nm of a membrane. Only BSA-gold particles within the limiting membrane of a compartment were counted. Percentages of gold particles present in each compartment are shown. Six types of endocytic compartments could be distinguished, each with a characteristic morphology, as shown in the table. The highest percentage of Tf-HRP is present in type 1 compartments, both after 3 and 10 min of incubation. Tf-HRP has not been detected in types 4, 5, and 6 to a significant extent. The quantitation of BSA-gold particles present in each of the compartments during the pulse–chase shows that at 3- and 10-min pulse only types 1, 2, and 3 are reached, whereas type 4, 5, and 6 compartments are sequentially reached by this tracer after 20- and 50-min chase.

Table II shows results of the quantitative evaluation of Tf-HRP and BSA-gold uptake in A20.A^b cells. The transport kinetics of Tf-HRP and BSA-gold were remarkably similar to those in 6H5.DM cells, with the exception that the later types 5/6 were more rapidly reached by BSA-gold, increasing from 10% immediately after 10-min pulse to 56% at 50-min chase. As in 6H5.DM cells, BSA-gold reached type 3 compartments immediately after 3 min of uptake (16%) and had increased to 38% after 10 plus 20 min. These data indicate that also in A20.A^b cells, types 1 through 5/6 were sequentially reached by BSA-gold and that types 1 and 2 represent EEs. Thus, as in the human cells, type 3 compartments displayed an intermediate position between the early types 1, 2, and the later 4 and 5/6 compartments.

Quantitative Distribution of Class II, I-Chain, and H-2M in A20.A^b Cells

Class II labeling was found in all types of endocytic compartments, except type 1. Fig. 3 *B* shows the quantitative

A

6H5.DM	type 1	type 2	type 3	type 4	type 5	type 6	total gold
DR	0	0	4	25	33	38	466
DM	0	0	5	22	26	47	241
I-Ab	0	1	2	12	43	42	853
YAe	0	0	11	27	39	23	148
IC	0	16	57	26	1	0	196
IN	0	14	38	42	6	0	99

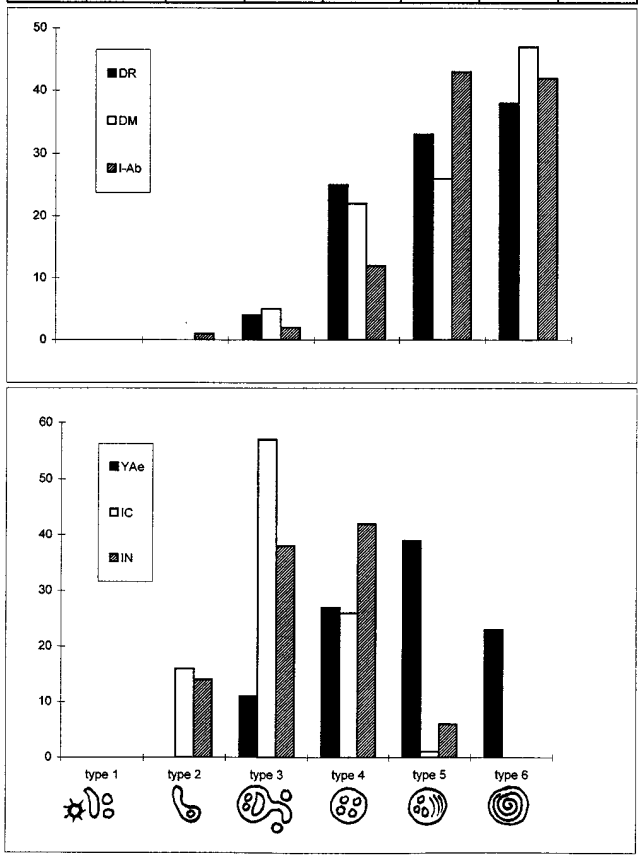

B

A20.Ab	type 1	type 2	type 3	type 4	type 5/6	total gold
CI-II	0	11	25	20	44	251
DM	0	2	7	29	63	189
IN	0	14	54	26	6	184

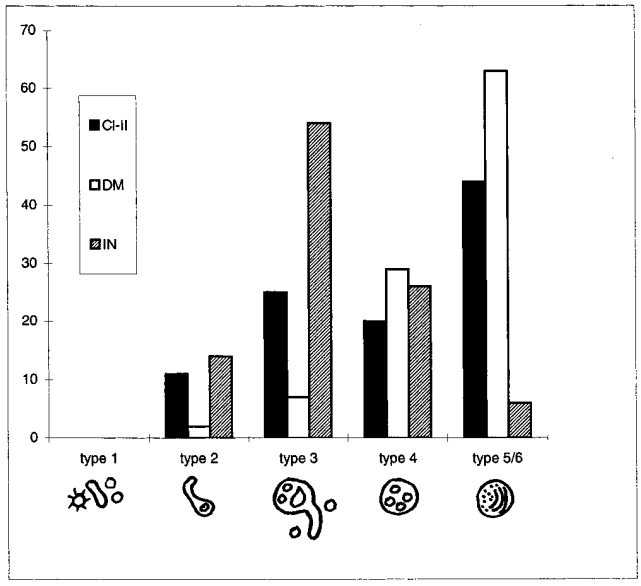

Figure 3. Quantitative analysis and graphical representation of Class II, DM, YA*e*, I-chain COOH terminus (*IC*), and I-chain NH_2 terminus (*IN*) distribution in endocytic compartments of 6H5.DM (*A*) and A20.A^b (*B*) cells. Ultrathin cryosections of 6H5.DM cells were single immunolabeled for the indicated molecules using 10-nm gold particles. For each immunolabeling, 20 cell profiles were randomly selected and gold particles were counted directly in the microscope. (*A*) In 6H5.DM cells, six types of endocytic compartments could be distinguished, and only these were subjected to quantitation. These compartments were identified by their morphological characteristics, as shown in the bottom of the figure. The percentages of gold particles present in each compartment are summarized in the table. The total number of gold particles counted is shown in the last column of the table. Percentages of labeling for DR, DM, and I-A^b (*top graph*) and of YA*e*, I-chain COOH terminus, and I-chain NH_2 terminus (*bottom graph*) are shown on the y axes. The graphs show strong enrichment of IC labeling in type 3 compartments, whereas labeling for DR, DM, and I-A^b is most abundant in types 5 and 6. IN labeling in types 3 and 4 is almost similar, while YA*e* is detected first in type 3 compartments and significantly enriched in the later types 4 to 6 (*B*). Quantitative analysis of A20.A^b cells was performed as described for 6H5.DM cells. I-chain NH_2 terminus is strongly enriched in type 3 compartments, and both class II and DM are abundant in type 4 and 5/6 compartments.

immunogold labeling data for class II, H-2M, and I-chain. More than 50% of the total I-chain labeling was found in type 3 compartments (illustrated in Fig. 6). I-chain was also present in type 2 (Fig. 4 *B*) and type 4 and to a much lower extent in type 5/6 (not illustrated). Of the total H2-M labeling only 2% was present in type 2 (Fig. 4 *E*), 7% in type 3, almost 30% in type 4, and 60% in type 5/6. Morphology, accessibility to exogenous tracers, and immunolabeling characteristics of type 3 MIICs were similar to those in 6H5.DM. YA*e* labeling was too low for demonstration with IEM. LAMP-1 was mainly present in type 5/6 compartments, similar to cathepsin D (Fig. 5 *B*). The type 5/6 compartments probably correspond to the late endocytic MIICs in human B lymphocytes (17, 37, 38). Some LAMP-1 was detected in type 3 (Fig. 5 *C*). Approximately 60% of the cathepsin D-positive endocytic compartments contained class II. MPR labeling was absent from any of the type 1 through 5/6 compartments and was primarily found in adjacent small vesicles and tubules (Fig. 5 *A*).

In conclusion, both human and mouse B cells displayed multiple types of class II-containing endocytic MIICs with internal membranes, including the early type of MIIC. Early MIICs are located just downstream of the major recycling EEs, contain DM molecules and abundant I-chain, and are the first endocytic compartments displaying class II–peptide complexes as recognized by YA*e* antibody. In both cell types we have not found any special class II-containing endocytic compartment apparent from the classical ones described above.

Discussion

This study expands on our previous work describing MIICs in B lymphoblasts, dendritic cells, and macrophages (for review see 24). In all of these cell types we have found late endocytic MIICs with similar morphological and molecular characteristics containing most of the intracellular class II molecules. However, over the years several reports have shown the transient presence of class II molecules in early endocytic compartments (1, 2, 6, 8, 13,

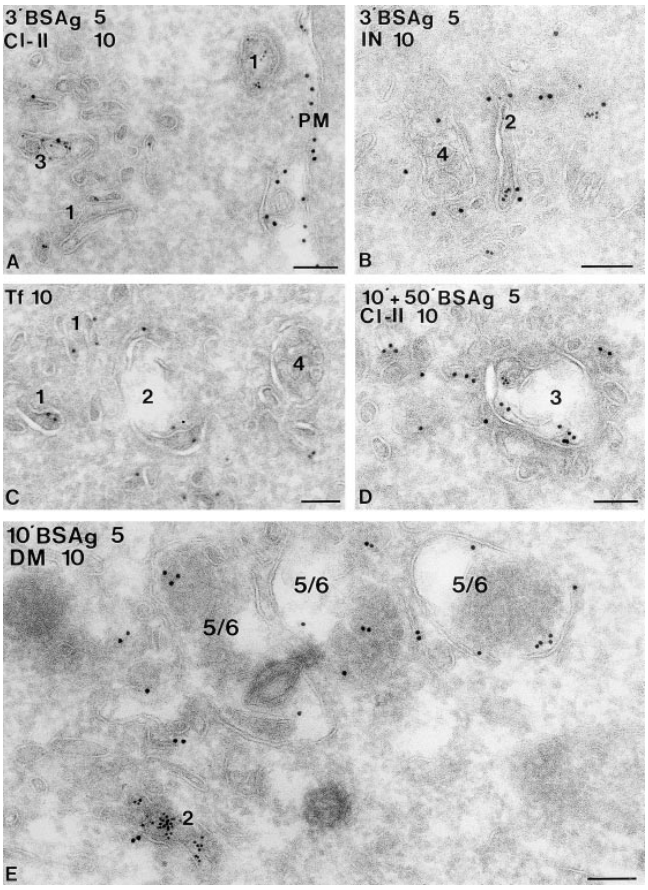

Figure 4. Endocytic compartments in A20.A^b cells. A20.A^b cells were incubated with 5-nm BSA-gold particles (*BSAg*) for 3 and 10 min (*A*, *B*, *D*, and *E*, respectively) or with Tf-HRP (*Tf*) for 10 min (*C*). After 3 min of BSA-gold uptake, particles are present in the type 1 compartment (*A*), which includes coated vesicles and some noncoated vesicles and tubules. BSA-gold is also present in the type 2 compartment at this time point (*B*) but is absent from the multivesicular type 4. In this picture, both types are immunolabeled for I-chain NH_2 terminus. A type 3 compartment, shown in *A* and *D*, exhibits BSA-gold both after 3 min and 10 plus 50 min of uptake. Class II is present in type 3 compartments (*A* and *D*), which show the typical irregularly shaped morphology and electron lucent content with few internal vesicles (*D*). Type 5/6 compartments (*E*), with a dense content and few internal membranes, do not show BSA-gold after 10 min of uptake, while the type 2 compartment is positive for BSA-gold. Labeling for H-2M (*DM*, 10-nm gold particles) reveals little H-2M in the type 2, whereas type 5/6 compartments are strongly labeled for H-2M. Bars, 100 nm.

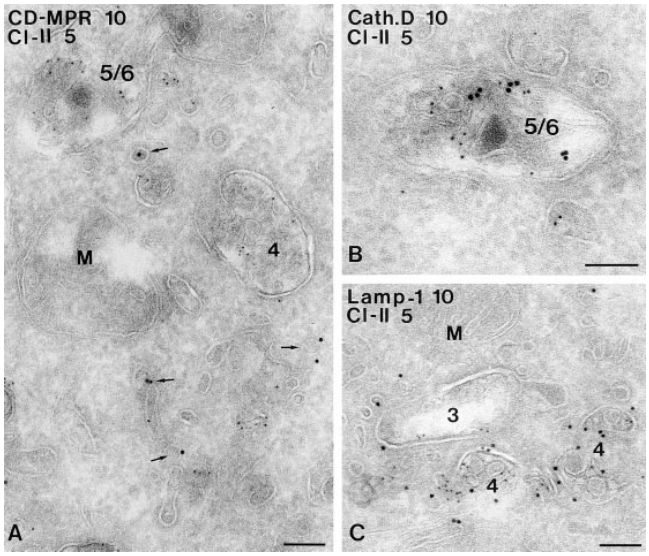

Figure 5. Characterization of MIICs in A20.A^b cells. Ultrathin cryosections of A20.A^b cells were double immunolabeled for class II and CD-MPR (*A*), cathepsin D (*B*), or LAMP-1 (*C*). Labeling for class II (5-nm gold particles) is present in type 4 and type 5/6 compartments (*A*), whereas CD-MPR labeling (10-nm gold particles) is detected only in small, dense vesicles (*arrows*). In *B*, a type 5/6 compartment positive for both class II (5-nm gold particles) and cathepsin D (10-nm gold particles) is shown. Labeling for LAMP-1 (10-nm gold particles) and class II (5-nm gold particles) is demonstrated in two multivesicular type 4 compartments (*C*). A type 3 compartment shown here contains some class II labeling, and only little LAMP-1 labeling. *M*, mitochondrion. Bars, 100 nm.

26, 48, 49, 58). The criteria used in the different studies to define early endocytic compartments varied, and their morphological identity was often not revealed. We have now studied for the first time in great detail the endocytic pathway of both mouse A20.A^b and human 6H5.DM B lymphoblasts, using semi-quantitative IEM.

Based on morphology, molecular marker distribution, and position in the endocytic pathway, six and five types of endocytic compartments could be distinguished in the 6H5.DM and A20.A^b cells, respectively (Tables I and II; Fig. 7). Pulse–chase endocytosis of Tf-HRP and BSA-gold indicated the position of these compartments in the endocytic pathway. Type 1, 2, and 3 compartments were situated early in the endocytic pathway. Types 1 and 2 represented the major Tf-recycling compartments and therefore most likely were classical EEs in these cells. Type 3 had

Table II. Quantitative Analysis of Tf-HRP and BSA-Gold Uptake in A20.A^b Cells

A20	Type 1	Type 2	Type 3	Type 4	Type 5/6
3 min Tf-HRP	74	21	5	–	–
10 min Tf-HRP	82	12	6	–	–
3 min BSA-gold	63	21	16	–	–
10 min BSA-gold	55	21	6	8	10
10 + 20 min BSA-gold	14	3	38	38	7
10 + 50 min BSA-gold	6	2	10	27	56

Experiments were performed as described in Table I. Only five types, compared to six types in 6H5.DM cells, showed morphologically distinguishable endocytic compartments in A20.A^b cells. The quantitation of gold particles for Tf-HRP in A20.A^b cells shows the abundant presence of Tf-HRP in type 1 compartments and lower amounts in types 2 and 3. After 3 min of BSA-gold uptake, the tracer is most prominently present in type 1, to some extent in type 2 and 3, but not in type 4 and 5/6 compartments. Already after 10 min of internalization, type 4 and 5/6 compartments contain significant amounts of BSA-gold, and these BSA-gold numbers increase after 20- and 50-min chase.

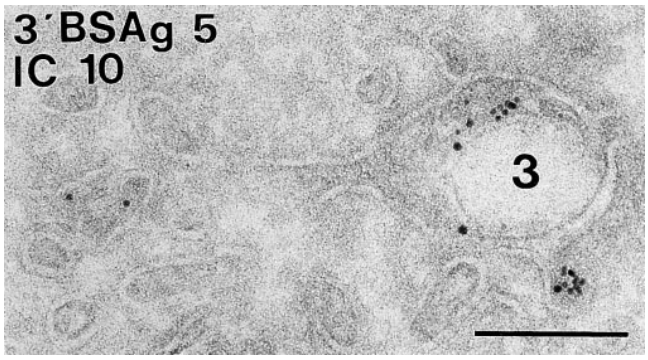

Figure 6. Immunogold labeling of I-chain in early MIICs of A20.A^b cells. A type 3/early MIIC with characteristic empty space is shown containing internalized BSA-gold particles and labeling for I-chain COOH terminus. Bar, 200 nm.

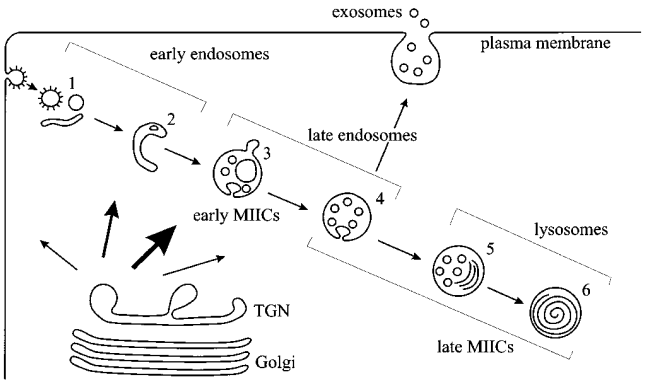

Figure 7. Comprehensive scheme of endocytic compartments and class II trafficking in B cells. The proposed relation between the different types of endocytic compartments (1–6) including early and late MIICs as described in this study, and the classical terminology of endosomes and lysosomes are indicated. From our present morphological observations and the kinetic data in several recent fractionation studies (see Discussion), the following model of class II transport can be put forward. Class II/I-chain complexes derived from the TGN are transported to early MIICs and possibly to a minor extent to the plasma membrane and other endocytic compartments (see *arrows with different thicknesses radiating from the TGN*). After arrival in the endocytic pathway, class II/I-chain complexes migrate farther down the endocytic route (see *arrows between types 1–6*) together with endocytosed antigens, meanwhile being exposed to increasing proteolytic activity. This activity results in the removal of I-chain, a process probably already starting in type 3/early MIICs and progressing in later compartments. Once class II is freed from the I-chain peptide CLIP, antigenic peptides can bind to the class II molecules, a process catalyzed by HLA-DM. Peptide loading of class II commences in early MIICs and proceeds in later compartments, possibly depending on the type of class II and antigen. Escape of class II–peptide complexes from the degradative route for deposition at the cell surface has been shown to occur by exocytosis of MIICs by which the limiting membrane of MIICs is incorporated in the plasma membrane. During this process the internal vesicles of MIICs are externalized as exosomes (43). Other pathways of class II/peptide transport to the cell surface may very well exist but have not yet been identified.

the characteristics of a transitional compartment between the types 1 and 2 and the later type 4 compartments. Abundance of I-chain, the presence of some Tf-HRP, rapid arrival of BSA-gold, irregular shape, and few internal vesicles characterized type 3 as early MIIC (17). As in our previous studies (for review see 24), most of the intracellular class II molecules were detected in type 4, 5, and 6 compartments, which represented LEs (type 4) and lysosomes (types 5 and 6), because of their marker profiles and because they were reached by internalized BSA-gold in sequence and after types 1, 2, and 3. The morphology of the multivesicular (type 4), intermediate (type 5), and multilaminar (type 6) as well as their late position in the endocytic pathway matched the characteristics of MIICs as originally defined (37). Types 5, 5/6, and 6 are probably classical dense lysosomes. We have not encountered any class II-positive endocytic structure distinct from the types above. Fig. 7 shows the possible functional connections between the various types of compartments and how the type numbers may correlate with existing nomenclature.

The labeling patterns for I-chain and YA*e* suggest that type 3/early MIICs are of particular interest with respect to class II function. First, early MIICs contained 40 and 55% of the I-chain labeling in the human and mouse cells, respectively. In types 4, 5, and 6, I-chain labeling progressively decreased, most likely due to progressive proteolysis. The abundance of I-chain COOH terminus epitope in early MIICs (17, 38, and this study) probably reflects both class II-bound and -detached I-chain. The sequential COOH- to NH_2-terminal degradation of I-chain likely accounts for the earlier disappearance of COOH terminus labeling than of NH_2 terminus labeling. An attractive interpretation of the I-chain labeling pattern is that early MIICs represent an important entry point of class II/I-chain molecules coming from the TGN. This would be in accordance with our previous observations (17, 38) and with those of Cresswell (8) and Castellino and Germain (6). However, in both the 6H5.DM and A20.A^b cells a small but significant fraction of I-chain was found in type 2 compartments. It is therefore likely that class II/I-chain complexes can enter the endocytic pathway even earlier, either directly from the TGN or via the plasma membrane (48, 49, 58, 63). This latter pathway is probably a minor one in human B cells, since major amounts of biosynthetically labeled class II molecules cotransport with pro-cathepsin D directly from the TGN to endosomes within the same vesicular intermediates (17). The fact that we found only low class II and abundant I-chain labeling in early MIICs is possibly due to differences in specificities and immunolabeling efficiencies of the antibodies used. In addition, epitopes recognized by the polyclonal antibody against human class II α-chain may partly be masked when associated with I-chain. Class II/I-chain complexes present in type 2 EEs may therefore have been underscored. Several recent subcellular fractionation studies on B cells have shown direct transport of αβ/I-chain complexes from the TGN to late MIIC-like compartments (32, 41, 57, 60). Our present morphological observations are broadly consistent with those of Castellino and Germain (6) who used a refractionation and density shift protocol on murine splenic B cells and found that most newly synthesized class II/I-chain complexes first enter EEs and then migrate farther down the endocytic system (see also 49). In their study, EEs were marked by labeling with HRP during 10 min of fluid phase endocytosis.

We have defined EEs by their Tf content after 3 min of receptor-mediated uptake. After 10 min of BSA-gold fluid phase uptake, tracer had already accessed early MIICs significantly (17, this study). It therefore seems likely that the EE subcellular fraction in the study of Castellino and Germain (6) included early MIICs. Mellman et al. (30) proposed a model in which class II/I-chain complexes are first transported to EEs for removal of I-chain, whereupon class II molecules are included in CIIVs that are formed from EEs by a distinct budding process.

A second important aspect of early MIICs is their possible involvement in peptide loading. Although the majority of the DRα52-68/I-A^b complexes, recognized by the YA*e* antibody, was found in type 4, 5, and 6 compartments (31), we now demonstrate the presence of the YA*e* epitope already in early MIICs. Early MIICs contain lysosomal enzymes so that degradation of I-chain and of endocytosed antigen may occur simultaneously here (17). Since early MIICs also harbor HLA-DM molecules, important requirements for antigen processing and peptide loading of class II molecules are met in this compartment. Appearance of antigen-presenting capacity after antigen uptake and acquisition of class II SDS stability, as indications of peptide loading, have led to the notion that late MIICs are the primary sites of peptide loading in macrophages and B cell lines (6, 21, 41, 60, 65). In human B lymphoblasts, West et al. (60) detected peptide loading activity first in a compartment distinct from early (Tf$^+$) and late (MPR$^+$) endosomes and with a morphology similar to MIICs. Recently it was shown that in addition, EEs can be involved in peptide loading (13, 18). Such an activity was dependent on the type of antigen used and, more interestingly, varied between different epitopes present in one particular antigen. According to Castellino and Germain (6), SDS-stable complexes present in EEs may also represent recycling class II–peptide complexes (40, 44, 46). Our quantitative IEM shows that at steady state a little more than 10% of an abundant endogenous class II–peptide complex is present in early MIICs but is undetectable in EEs. However, most of the complexes were found in late MIICs, which may have accumulated there after traversing the endocytic pathway and/or represent complexes formed de novo in later compartments. We have not found YA*e* labeling in any other type of vesicle, distinct from early and late MIICs, which argues against the possible existence of a unique compartment serving as the exclusive assembly site of class II–peptide complexes.

Although the endocytic compartments of 6H5.DM and A20.A^b cells were very similar in most of their characteristics, several differences were noted. 6H5.DM cells contained many multilaminar MIICs (type 6), while A20.A^b cells were mostly devoid of this MIIC type as well as of the intermediate MIICs (type 5). In their place, a dense MIIC (type 5/6) with only few internal membranes was prominently present. Thus, the multilaminar structure may not be the most discriminative morphological feature of MIICs in general. We have previously detected dense instead of multilaminar MIICs in dendritic cells from skin and spleen (22, 23). In 6H5.DM cells, 95% of the 4–6 types of endocytic structures contained class II molecules, in contrast to 60% in A20.A^b cells. Furthermore, sections of 6H5.DM cells showed twice as many profiles of endocytic organelles than A20.A^b cells. A20.A^b cells have been reported to contain <5% of their total class II molecules intracellularly (1) versus up to 36% in human B cells (17). Together these data illustrate that the A20.A^b cells exhibit relatively poorly developed intracellular antigen processing and binding organelles, a feature that may hold for other mouse B cells as well (M.J. Kleijmeer, unpublished observations).

A most puzzling question concerns the relationship between CIIVs in mouse A20 cells (30) and MIICs defined in several human and mouse APCs (24). As far as we could test by IEM, our A20.A^b did not contain a distinct structure with all the characteristics reported for CIIVs. Nevertheless, many CIIV features matched those of early MIICs. Like CIIVs, early MIICs were not a major station in the Tf-recycling pathway, were markedly distinct from LEs and lysosomes, and contained peptide-loaded class II molecules. Furthermore, CIIV-enriched fractions were described to contain multivesicular structures (1) reminiscent of type 3 and 4 compartments in the present study. In addition, HLA-DM occurred only at relatively low levels in both early MIICs (this study) and CIIVs (39). On the other hand, while CIIVs were the predominant location of intracellular class II molecules and appeared to serve as an exclusive site for compact forms of class II (2), we found only 25% of the intracellular class II molecules in early MIICs of A20.A^b cells and most in the later MIICs. A possible explanation for this could be that we have used A20 cells transfected with I-A^b. Since the M5/114 antibody recognizes both I-A^b and I-A^d, overexpression of one may have caused a shift to additional late endocytic compartments in our study. In both 6H5.DM and A20.A^b cells the most striking feature of early MIICs was the enrichment in I-chain. This feature differs markedly from the low I-chain content reported for CIIVs (1, 2). It should be noted, however, that this may partly be caused by the specificity of antibody MKD6 used by Amigorena et al. (1), which does not efficiently recognize class II/I-chain complexes (5). Finally, since CIIVs were isolated by free-flow electrophoresis, they may represent a subset of early endocytic membranes that, because of their charge, show a unique deflection pattern.

In conclusion, our present observations show a major fraction of I-chain present in early MIICs, positioned just downstream of EEs. Most of the class II and HLA-DM molecules distribute to typical late endosomal/lysosomal MIICs (Fig. 7). Thus, MIICs appear to represent a heterogenous set of conventional late and lysosomal compartments, identical to their counterparts in non-APCs. The current, poorly defined connotations of EE, LE, and lysosome are insufficient to describe what we can distinguish in the endocytic pathway of class II by IEM. Since understanding of these compartments and the relationships between them is still incomplete, the term MIIC continues to be a convenient designation. We propose that APCs employ their full endocytic system for antigen processing and loading, which would enable them to process both easily degradable and proteolytically resistant antigens into peptides shortly or late after antigen uptake.

We would like to thank Dr. G. Raposo for helpful discussions, and R. Scriwanek is gratefully acknowledged for his excellent photographical work.

This work was supported by the Dutch Organization of Scientific Research (NWO) grant 901-09-241.

Received for publication 17 February 1997 and in revised form 22 August 1997.

References

1. Amigorena, S., J.R. Drake, P. Webster, and I. Mellman. 1994. Transient accumulation of new class II MHC molecules in a novel endocytic compartment in B lymphocytes. *Nature (Lond.).* 369:113–120.
2. Amigorena, S., P. Webster, J. Drake, J. Newcomb, P. Cresswell, and I. Mellman. 1995. Invariant chain cleavage and peptide-loading in major histocompatibility complex class II vesicles. *J. Exp. Med.* 181:1729–1741.
3. Bénaroche, P., M. Yilla, G. Raposo, K. Ito, K. Miwa, H.J. Geuze, and H.L. Ploegh. 1995. How MHC class II molecules reach the endocytic pathway. *EMBO (Eur. Mol. Biol. Organ.) J.* 14:37–49.
4. Bhattacharya, A., M.E. Dorf, and T.A. Springer. 1981. A shared alloantigenic determinant on Ia antigens encoded by the I-A and I-E subregions: evidence for I region gene duplication. *J. Immunol.* 127:2488–2495.
5. Bikoff, E.K., R.N. Germain, and E.J. Robertson. 1995. Allelic differences affecting invariant chain dependency of MHC class II subunit assembly. *Immunity.* 2:301–310.
6. Castellino, F., and R.N. Germain. 1995. Extensive trafficking of MHC class II-invariant chain complexes in the endocytic pathway and appearance of peptide-loaded class II in multiple endocytic compartments. *Immunity.* 2: 73–88.
7. Chen, J.W., T.L. Murphy, M.C. Willingham, J.T. Pastan, and J.T. August. 1985. Identification of two lysosomal membrane glycoproteins. *J. Cell Biol.* 101:85–95.
8. Cresswell, P. 1985. Intracellular class II HLA antigens are accessible to transferrin-neuraminidase conjugates internalized by receptor-mediated endocytosis. *Proc. Natl. Acad. Sci. USA.* 82:8188–8192.
9. Cresswell, P. 1994. Assembly, transport, and function of MHC class II molecules. *Annu. Rev. Immunol.* 12:259–293.
10. Davidson, H.W., and C. Watts. 1989. Epitope-directed processing of specific antigens by B-lymphocytes. *J. Cell Biol.* 109:85–92.
11. Denzin, L.K., and P. Cresswell. 1995. HLA-DM induces CLIP dissociation from MHC class II αβ dimers and facilitates peptide-loading. *Cell.* 82: 155–165.
12. Eastman, S., M. Deftos, P. de Roos, D.H. Hsu, L. Teyton, N.S. Braunstein, C.J. Hackett, and A.Y. Rudensky. 1996. A study of the assembly of invariant chain peptide: MHC class II complexes using a new complex-specific monoclonal antibody. *Eur. J. Immunol.* 26:385–393.
13. Escola, J.-M., J.-C. Grivel, P. Chavrier, and J.-P. Gorvel. 1995. Different endocytic compartments are involved in the tight association of class II molecules with processed hen egg lysozyme and ribsnuclease A in B-cells. *J. Cell Sci.* 108:2337–2345.
14. Germain, R.N., and D.H. Margulies. 1993. The biochemistry and cell biology of antigen processing and presentation. *Annu. Rev. Immunol.* 11: 403–450.
15. Geuze, H.J., J.W. Slot, P.A. van der Ley, and R.C.T. Scheffer. 1981. Use of colloidal gold particles in double-labeling immunoelectron microscopy of ultrathin frozen tissue sections. *J. Cell Biol.* 89:653–665.
16. Geuze, H.J., W. Stoorvogel, G.J. Strous, J.E. Bleekemolen, and I. Mellman. 1988. Sorting of mannose 6-phosphate receptors and lysosomal membrane proteins in endocytic vesicles. *J. Cell Biol.* 107:2491–2501.
17. Glickman, J.N., P.A. Morton, J.W. Slot, S. Kornfeld, and H.J. Geuze. 1996. The biogenesis of the MHC class II compartment in human I-cell disease B-lymphoblasts. *J. Cell Biol.* 132:769–785.
18. Griffin, J.P., R. Chu, and C.V. Harding. 1997. Early endosomes and late endocytic compartments generate different peptide/class II MHC complexes via distinct processing mechanisms. *J. Immunol.* 158:1523–1532.
19. Griffiths, G., B. Hoflack, K. Simons, I. Mellman, and S. Kornfeld. 1988. The mannose 6-phosphate receptor and the biogenesis of lysosomes. *Cell.* 53:329–341.
20. Harding, C.V., and H.J. Geuze. 1993. Immunogenic peptides bind to class II compartments in an early lysosomal compartment. *J. Immunol.* 151: 3988–3998.
21. Hunziker, W., and H.J. Geuze. 1996. Intracellular trafficking of lysosomal membrane proteins. *Bioessays.* 18:379–389.
22. Kleijmeer, M.J., V.M.J. Oorschot, and H.J. Geuze. 1994. Human resident Langerhans cells display a lysosomal compartment enriched in MHC class II. *J. Investig. Dermatol.* 103:516–523.
23. Kleijmeer, M.J., M.A. Ossevoort, C.J.H. van Veen, J.J. van Hellemond, J.J. Neefjes, W.M. Kast, C.J.M. Melief, and H.J. Geuze. 1995. MHC class II compartments and the kinetics of antigen presentation in activated mouse spleen dendritic cells. *J. Immunol.* 154:5715–5724.
24. Kleijmeer, M.J., G. Raposo, and H.J. Geuze. 1996. Characterization of MHC class II compartments by immunoelectron microscopy. *Methods.* 10:191–207.
25. Klumperman, J., A. Hille, T. Veenendaal, V. Oorschot, W. Stoorvogel, K. von Figura, and H.J. Geuze. 1993. Differences in the endosomal distributions of the two mannose 6-phosphate receptors. *J. Cell Biol.* 121:997–1010.
26. Koch, N., S. Koch, and G.J. Hämmerling. 1982. Ia invariant chain detected on lymphocyte surfaces by monoclonal antibody. *Nature (Lond.).* 299: 644–645.
27. Koch, S., A. Schultz and N. Koch. 1987. The production of recombinant HLA-DRβ and invariant chain polypeptides by cDNA expression in *E. coli. J. Immunol. Methods.* 203:211–220.
28. Liou, W., H.J. Geuze, and J.W. Slot. 1996. Improved structural integrity of cryosections for immunogold labeling. *Histochem. Cell Biol.* 106:41–58.
29. Mellman, I. 1996. Endocytosis and molecular sorting. *Annu. Rev. Dev. Biol.* 12:575–625.
30. Mellman, I., P. Pierre, and S. Amigorena. 1995. Lonely MHC molecules seeking immunogenic peptides for meaningful relationships. *Curr. Opin. Cell Biol.* 7:564–572.
31. Morkowski, S., G. Raposo, M.J. Kleijmeer, H.J. Geuze, and A.Y. Rudensky. 1997. Assembly of an abundant endogenous MHC class II: peptide complex in MHC class II compartments. *Eur. J. Immunol.* 27:609–617.
32. Morton, P.A., M.L. Zacheis, K.S. Giacoletto, J.A. Manning, and B.D. Schwartz. 1995. Delivery of nascent MHC class II-invariant chain complexes to lysosomal compartments and proteolysis of invariant chain by cysteine proteases precedes peptide binding in B-lymphoblastoid cells. *J. Immunol.* 154:137–150.
33. Murphy, D.B., D. Lo, S. Rath, R.L. Brinster, R.A. Flavell, A. Slanetz, and C.A. Janeway, Jr. 1989. A novel MHC class II epitope expressed in thymic medulla but not in cortex. *Nature (Lond.).* 338:765–767.
34. Neefjes, J.J., V. Stollorz, P.J. Peters, H.J. Geuze, and H.L. Ploegh. 1990. The biosynthetic pathway of MHC class II but not class I molecules intersects with the endocytic route. *Cell.* 61:171–183.
35. Nijman, H.W., M.J. Kleijmeer, M.A. Ossevoort, V.M.J. Oorschot, M.P.M. Vierboom, M. van de Keur, P. Kenemans, W.M. Kast, H.J. Geuze, and C.M.J. Melief. 1995. Antigen capture and MHC class II compartments of freshly isolated and cultured human blood dendritic cells. *J. Exp. Med.* 182:163–174.
36. Odorizzi, C.G., I.S. Trowbridge, L. Xue, C.R. Hopkins, C.D. Davis, and J.F. Collawn. 1994. Sorting signals in the MHC class II invariant chain cytoplasmic tail and transmembrane region determine trafficking to an endocytic processing compartment. *J. Cell Biol.* 126:317–330.
37. Peters, P.J., J.J. Neefjes, V. Oorschot, H.L. Ploegh, and H.J. Geuze. 1991. Segregation of MHC class II molecules from MHC class I molecules in the Golgi complex for transport to lysosomal compartments. *Nature (Lond.).* 349:669–676.
38. Peters, P.J., G. Raposo, J.J. Neefjes, V. Oorschot, R.L. Leyendekker, H.J. Geuze, and H.L. Ploegh. 1995. Major histocompatibility complex class II compartments in human B-lymphoblastoid cells are distinct from early endosomes. *J. Exp. Med.* 182:325–334.
39. Pierre, P., L.L. Denzin, C. Hammond, J.R. Drake, S. Amogorena, P. Cresswell, and I. Mellman. 1996. HLA-DM is localized to conventional and unconventional MHC class II-containing endocytic compartments. *Immunity.* 4:229–239.
40. Pinet, V., M. Vergelli, R. Martin, O. Bakke, and E.O. Long. 1995. Antigen presentation mediated by recycling of surface HLA-DR molecules. *Nature (Lond.).* 375:603–606.
41. Qiu, Y., X. Xu, A. Wandinger-Ness, D.P. Dalke, and S.K. Pierce. 1994. Separation of subcellular compartments containing distinct functional forms of MHC class II. *J. Cell Biol.* 125:595–605.
42. Ramachandra, L., S. Kovats, and A.Y. Rudensky. 1996. Variation in HLA-DM expression influences conversion of MHC class II αβ:class II-associated invariant chain peptide complexes to mature peptide-bound class II αβ dimers in a normal B-cell line. *J. Immunol.* 156:2196–2204.
43. Raposo, G., H.W. Nijman, W. Stoorvogel, R.L. Leyendekker, C.V. Harding, C.J.M. Melief, and H.J. Geuze. 1996. B lymphocytes secrete antigen presenting vesicles. *J. Exp. Med.* 183:1–12.
44. Reid, P.A., and C. Watts. 1990. Cycling of cell-surface MHC glycoprotein through primaquine-sensitive intracellular compartments. *Nature (Lond.).* 346:655–657.
45. Roche, P.A. 1995. HLA-DM: an in vivo facilitator of MHC class II peptide-loading. *Immunity.* 3:259–262.
46. Roche, P.A., and P. Cresswell. 1990. Invariant chain association with HLA-DR molecules inhibits immunogenic peptide binding. *Nature (Lond.).* 345: 615–618.
47. Roche, P.A., and P. Cresswell. 1991. Processing of the class II-associated invariant chain generates a peptide binding site in intracellular HLA-DR molecules. *Proc. Natl. Acad. Sci. USA.* 88:3150–3154.
48. Roche, P.A., C.L. Teletski, E. Stang, O. Bakke, and E.O. Long. 1993. Cell surface HLA-DR-invariant chain complexes are targeted to endosomes by rapid internalization. *Proc. Natl. Acad. Sci. USA.* 90:8581–9585.
49. Romagnoli, P., C. Layet, J. Yewdell, O. Bakke, and R.N. Germain. 1993. Relationship between invariant chain expression and major histocompatibility complex class II transport into early and late endocytic compartments. *J. Exp. Med.* 177:583–596.
50. Rudensky, A.Y., P. Preston-Hurlburt, S.C. Hong, A. Barlow, and C.A. Janeway, Jr. 1991. Sequence analysis of peptides bound to MHC class II molecules. *Nature (Lond.).* 353:622–628.
51. Rudensky, A.Y., M. Maric, E. Eastman, L. Shoemaker, P.C. de Roos, and J.S. Blum. 1994. Intracellular assembly and transport of endogenous peptide: MHC class II complexes. *Immunity.* 1:585–594.
52. Sanderson, F., M.J. Kleijmeer, A. Kelly, D. Verwoerd, A. Tulp, J.J. Neefjes, H.J. Geuze, and J. Trowsdale. 1994. DM, an HLA-class II mole-

cule with an accessory function in antigen presentation, accumulates in an intracellular class II compartment. *Science (Wash. DC).* 266:1566–1569.
53. Schmid, S.L., and M.R. Jackson. 1994. Making class II presentable. *Nature (Lond.).* 369:103–104.
54. Slot, J.W., H.J. Geuze, and A.J. Weerkamp. 1988. Localization of macromolecular components by application of the immunogold technique on cryosected bacteria. *Methods Microbiol.* 21:211–236.
55. Stoorvogel, W., H.J. Geuze, J.M. Griffith, A.L. Schwartz, and G.J. Strous. 1989. Relations between the intracellular pathways of the receptor for transferin, asialoglycoprotein, and mannose 6-phosphate in human hepatoma cells. *J. Cell Biol.* 108:2137–2142.
56. Teyton, L., D. O'Sullivan, P.W. Dickson, V. Lotteau, A. Sette, P. Fink, and P.A. Peterson. 1990. Invariant chain distinguishes between the exogenous and endogenous presentation pathways. *Nature (Lond.).* 348:39–44.
57. Tulp, A., D. Verwoerd, B. Dobberstein, H.L. Ploegh, and J. Pieters. 1994. Isolation and characterization of the intracellular MHC class II compartment. *Nature (Lond.).* 369:120–126.
58. Warmerdam, P.A.M., E. Long, and P.A. Roche. 1996. Isoforms of the invariant chain regulate transport of MHC class II molecules to antigen processing compartments. *J. Cell Biol.* 133:281–291.
59. Watts, C. 1997. Capture and processing of exogenous antigens to presentation on MHC molecules. *Annu. Rev. Immunol.* 15:821–850.
60. West, M.A., J.M. Lucocq, and C. Watts. 1994. Antigen processsing and class II MHC peptide-loading compartments in human B-lymphoblastoid cells. *Nature (Lond.).* 369:147–151.
61. Williams, M.A., and M. Fukuda. 1990. Accumulation of lysosomal membrane glycoproteins in lysosomes requires a tyrosine residue at a particular position in the cytoplasmic tail. *J. Cell Biol.* 111:955–966.
62. Wolf, P.R., and H.L. Ploegh, 1995. How MHC class II molecules acquire peptide-cargo: biosynthesis and trafficking through the endocytic pathway. *Annu. Rev. Cell Dev. Biol.* 11:267–306.
63. Wraight, C.J., P. van Endert, P. Moller, J. Lipp, N.R. Ling, I.C.M. MacLennan, N. Koch, and G. Moldenhauer. 1990. Human major histocompatibility complex class II invariant chain is expressed on the cell surface. *J. Biol. Chem.* 265:5787–5792.
64. Wubbolts, R., M. Fernandez-Borja, L. Oomen, D. Verwoerd, H. Janssen, J. Calafat, A. Tulp, S. Dusseljee, and J.J. Neefjes. 1996. Direct vesicular transport of MHC class II molecules from lysosomal structures to the cell surface. *J. Cell Biol.* 135:611–622.
65. Xu, X., W. Song, H. Cho, Y. Qiu, and S.K. Pierce. 1995. Intracellular transport of invariant chain-MHC class II complexes to the peptide-loading compartment. *J. Immunol.* 155:2984–2992.